Communication
doi.org/10.1002/chem.202000663
Chemistry Europe
European Chemical Societies Publishing

Layered Compounds

A Layered Tin Bismuth Selenide with Three Different Building Blocks that Account for an Extremely Large Lattice Parameter of 283 Å

Markus Nentwig,[a] Lucien Eisenburger,[b] Frank Heinke,[a] Daniel Souchay,[a] and Oliver Oeckler*[a]

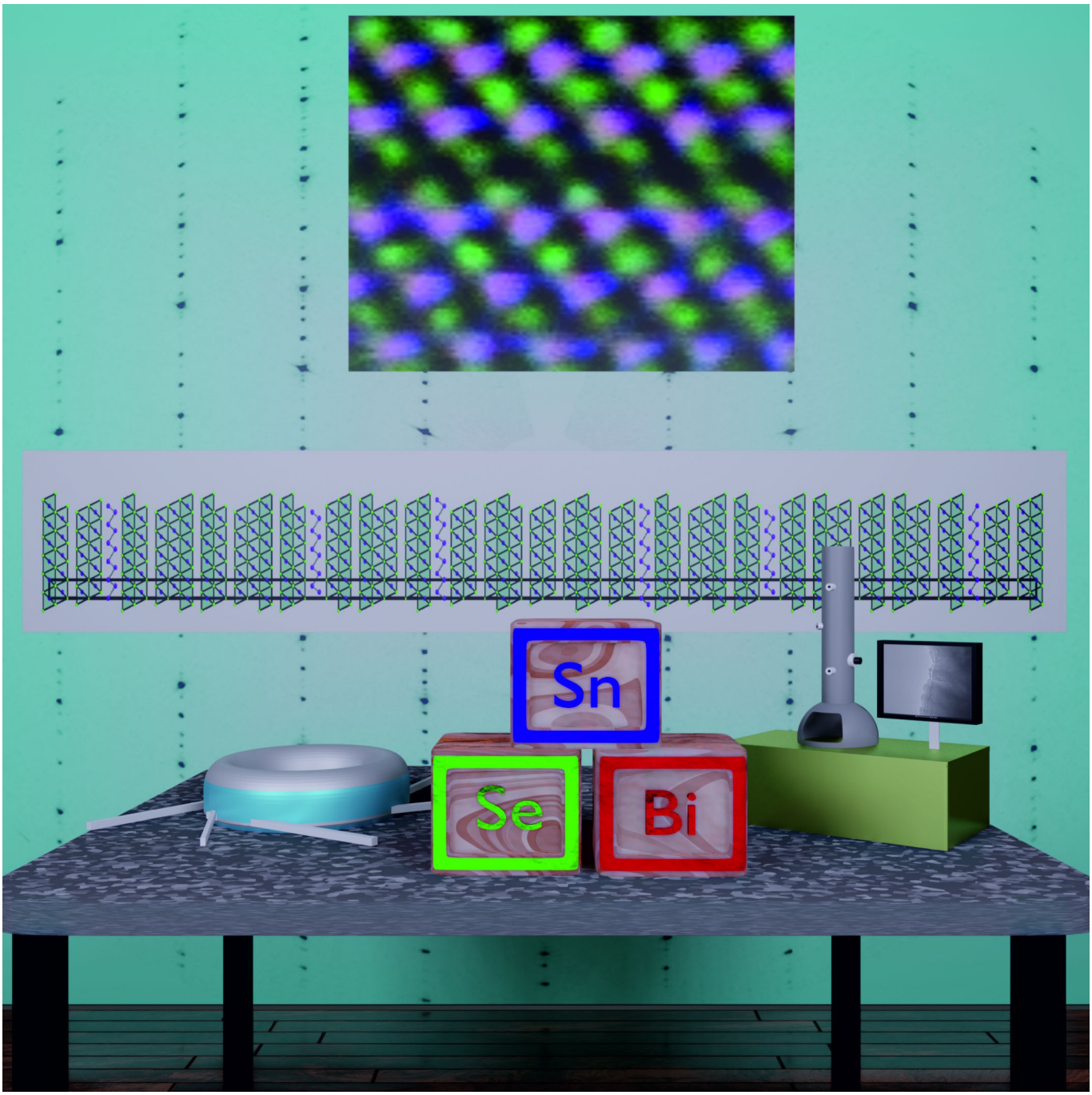

Abstract: The layered compound $Sn_{2.8(4)}Bi_{20.2(4)}Se_{27}$ exhibits an extraordinarily long-periodic 150*R* stacking sequence. The crystal structure contains three different building blocks, which form upon the addition of Sn to a Bi-rich bismuth selenide. Sn-doped Bi_2 double ("2") layers similar to those in elemental bismuth, $Sn_{0.3}Bi_{1.7}Se_3$ quintuple ("5") layers and $Sn_{0.4}Bi_{2.6}Se_4$ septuple ("7") layers are arranged in a 7525757525|7525757525|7525757525 sequence, which corresponds to a structure with $a = 4.1819(4)$ and $c = 282.64(6)$ Å in space group $R\bar{3}m$. The structure of a microcrystal was determined using microfocused synchrotron radiation and refined as a formally commensurately modulated structure in (3+1)D superspace (superspace group $R\bar{3}m(00\gamma)00$), with a trivial basic structure that contains just one atom. The stacking sequence as well as the cation distribution are confirmed by aberration-corrected scanning transmission electron microscopy (STEM) in combination with chemical mapping by X-ray spectroscopy with atomic resolution. Stacking faults are not typical but have been observed occasionally.

Owing to their pronounced compositional and structural diversity, chalcogenides represent one of the most intriguing classes of compounds in solid-state chemistry and physics.[1] Besides Bi_2Se_3, which is one of the most well-known topological insulators,[2] recent studies of for example, Bi_2Te_3,[3] $MnBi_2Te_4$,[4] and $SnBi_2Te_4$,[5] revealed their potential as topologically non-trivial materials. In addition, layered chalcogenides like BiSe,[6] SnSe,[7] and Bi-doped SnSe,[8] have attracted much attention in the field of thermoelectrics. Such chalcogenides also constitute a fascinating field of fundamental research. For example, single-crystal data of Ge_4Se_3Te revealed unexpected Ge–Ge bonds, which have been confirmed by STEM (scanning transmission electron microscopy) and theoretical calculations.[9] Modular stacking can lead to new inorganic-organic hybrid materials, for example, by inserting polymer chains in tin selenides.[10]

Layered chalcogenides often form homologous series of compounds, where variations of the slab thicknesses between van der Waals gaps characterize a plethora of new phases.[11] This can lead to compounds with large lattice parameters, which can be expected to be beneficial for thermoelectric properties as phonon scattering on the nanometer scale decreases thermal conductivity.[12] Compounds in the binary *M*/*X* systems with *M* = Sb, Bi and *X* = Se, Te form trigonal layered structures built up from M_2 double layers (symbolized by "2")—comparable to those in the element structures of Sb and Bi—and tetradymite-like M_2X_3 quintuple blocks symbolized by "5". Complex stacking results in large lattice parameters, for example, $c = 103$ Å for Bi_8Te_9, which features a 2555|2555|2555 sequence.[13] So far, no single-crystal X-ray data have been reported for such layered chalcogenides with long-periodic stacking sequences that exhibit lattice parameters larger than these 103 Å. Electron diffraction data and high-resolution transmission electron microscopy (HRTEM) of quenched samples, however, showed the presence of a rhombohedral bismuth telluride $Bi_{2+\delta}Te_3$ with a 138*R*-type stacking sequence ($\delta \approx 0.11$–0.75, $c \approx 275$ Å) of 55525552552|55525552552|55525552552.[14] In ternary systems such as $TtTe(Bi_2Te_3)_n$ (*Tt* = Ge, Sn, Pb), the structural chemistry is extended by building blocks with septuple ("7") $TtBi_2Te_4$ slabs in addition to quintuple ("5") Bi_2Te_3 slabs.[15] The structure with the longest periodicity has been found in a 159*R*-type germanium bismuth telluride that exhibits a 557575757|557575757|557575757 stacking sequence with $c \approx 318$ Å as deduced from electron diffraction patterns.[16] However, crystal structure refinements have not been reported for such extreme cases.

With respect to inorganic compounds, unit-cell dimensions of more than 100 Å are very unusual in general. They have been reported for a few binary compounds like the well-known polytypes of SiC,[17] ZnS,[18] CdI_2,[19] and PbI_2.[20] Varying sequences and orientations of the same structural entities result in polytypes with huge lattice parameters of up to 990 Å in SiC.[21] Such crystallographic phenomena have usually been observed only in small domains by electron microscopy; and the structures were assigned by plausibility or trial and error methods in case diffraction data were available. Only very few actual structure refinements based on single-crystal data of structure models with very large lattice parameters do exist. In this respect, even lattice parameters of around 57 Å as recently observed for cesium rare-earth silicates $Cs_3RESi_6O_{15}$ (*RE* = Dy-Lu, Y, In) have been reported as being unusually large,[22] although for example, for the mineral turtmannite with $c = 204$ Å, a full structure refinement has been carried out.[23] Hexaferrites are also prone to form anisotropic structures with large translation periods along the stacking direction of Ba-rich and Fe-rich slabs, which can be arranged with varying sequences that exhibit translation periods of up to 1577 Å for $Ba_{70}Zn_{66}Fe_{444}O_{802}$.[24] While this extraordinary layer stacking has only been identified by electron microscopy, Rosseinsky et al. fully refined the crystal structure of Ba/Fe/Zn oxide hexaferrite polytypes, for example, $Ba_{10}Fe_{72}Zn_8O_{126}$ with $c = 488$ Å, from single-crystal synchrotron data.[25] Hexaferrites can be identified by the 00*l* reflections in electron diffraction patterns and described by a unified (3+1)D superspace model.[26] Similar descriptions have been reported for perovskite-like compounds.[27] Lidin et al. developed a similar superspace formal-

[a] *M. Nentwig, Dr. F. Heinke, Dr. D. Souchay, Prof. Dr. O. Oeckler*
Institute for Mineralogy, Crystallography and Materials Science
Leipzig University
Scharnhorststraße 20, 04275 Leipzig (Germany)
E-mail: oliver.oeckler@gmx.de

[b] *L. Eisenburger*
University of Munich (LMU)
Department of Chemistry
Butenandtstraße 5-13, 81377 Munich (Germany)

Supporting information and the ORCID identification number(s) for the author(s) of this article can be found under: https://doi.org/10.1002/chem.202000663.

ism for the system Bi/Se described above.[28] Such superspace descriptions are well known from modulated structures, but the (3+1)D description of long-periodic layered structures does not mean that a somehow simpler structure is modified by wave-like displacements or occupation modulations. in fact, the hypothetical basic structure would consist of just one or a few atoms. Therefore, the superspace formalism focuses, on the one hand, on a unified description of a series of compounds. On the other hand, it gives access to elegant structure refinements in cases where the reflections of extremely large unit cells are too closely spaced to be integrated from area-detector data based on a 3D periodic indexing.

In the pseudobinary system $(SnSe)_xBi_2Se_3$, compounds with very diverse structures are formed.[29] Besides cubic $Sn_4Bi_2Se_7$ ($x=4$) with defect NaCl-type structure, and layered $SnBi_4Se_7$ ($x=0.5$) with defect $GeSb_2Te_4$-type structure, at least four compounds ($0.8\leq x\leq 3$) with structures derived from lillianite ($Pb_3Bi_2S_6$)[30] have been discovered. Here we report the single-crystal structure of a new compound in the system Sn/Bi/Se, which features an extraordinarily long lattice parameter of $c=$ 282.6 Å in a 150*R* stacking sequence.

A complex layered phase with the chemical composition $Sn_{2.8(4)}Bi_{20.2(4)}Se_{27}$ was formed during the decomposition of samples of $SnBi_4Se_7$ with defect $GeSb_2Te_4$-type structure.[29] The fact that this decomposition occurred during repeated slow heating indicates that the new phase is most likely thermodynamically stable at temperatures below $\approx$500 °C. The heterogeneous product was examined by scanning electron microscopy (SEM) and energy-dispersive X-ray spectroscopy (EDX), which revealed regions of different contrast and composition (Figure S1 and Table S1, "S" denotes Figures and Tables in the Supporting Information). In addition to a minority phase, which according to EDX corresponds to $Sn_{11.49}Bi_{12.39}Se_{30}$,[29] and a main phase of $Sn_{0.85}Bi_{2.15}Se_4$,[29] the title compound has been identified as a main component that is slightly Sn-depleted compared to the nominal composition $SnBi_4Se_7$.

A single crystal (Figure S2) of this unknown phase has been characterized by transmission electron microscopy (TEM) and EDX (Table S2). Using a fluorescence detector, this crystallite has been centered in a microfocused synchrotron beam at the European Synchrotron Radiation Facility (ESRF) and single-crystal diffraction data were recorded.[31] The crystallite exhibits a complex diffraction pattern. Initial attempts to determine the crystal structure from the single-crystal data by "routine data processing" resulted in a structure close to that of BiSe.[32] However, the fact that 60% of all reflections remained unindexed indicated that this was a wrong model. Taking into account the precise positions of the reflections leads to a unit cell with $c=282.6(6)$ Å; however, reasonable data cannot be extracted as many very weak reflections lie very close to strong ones that impede intensity integration. This problem can be overcome by formally describing the diffraction pattern based on the (3+1) dimensional superspace group $R\bar{3}m(00\gamma)00$. This involves a formal basic cell of $a=4.1819(4)$ and $c=5.6528(5)$ Å, which contains just one atom, with a commensurate modulation vector $q=87/50=1.74$. This way, all reflections in the reciprocal lattice can be indexed (Figure S3–S5). Following the concept outlined by Lidin et al.,[28] the structure solution and refinement were based on modulation parameters of the single atom site at the origin of the small unit cell of the basic structure (for details on the refinement see the Supporting Information). Initially assuming one Bi and one Se atom on this site, both fully occupied, the additional dimension in (3+1)D superspace can be used to modulate the occupancy using discontinuous functions. Crenel functions were used to describe the occupancy modulation by defining intervals in the additional dimension x4 where the corresponding atom exists. The refinement of the crenel function width Δ defines the overall chemical composition.

The refined value of $\Delta[Se1]=1-\Delta[Bi1]=0.5398(2)$ was constrained to 0.54 in order to provide an integer number of atoms in the unit cell. The resulting sum formula $Bi_{0.46}Se_{0.54}$ and a *q-vector* of $q=1.74=87/50$ correspond to a commensurate structure with a stacking sequence of 7525757525|7525757525|7525757525 (Figure 1). A refinement of positional modulation waves for Se and Bi shows their displacements along [001] (×3 direction), which became obvious from F_{obs} Fourier maps (Figure S6). Mixed occupancy of Sn and Bi was taken into account by a further modulation of site occupancy factors, again constrained to full occupancy. The refinement reveals a varying Sn fraction on the cation sites. The occupancy of the atoms as a function of the *t* variable in superspace (Figure S7) shows where the atoms are present in the ×4 dimension. The Sn fraction amounts to 4% in the double layers, whose structure corresponds to that of elemental Bi, up to 16% at the central position in septuple layer (Figure S8). This results in a sum formula of $Sn_{2.8(4)}Bi_{20.2(4)}Se_{27}$, well in line with the EDX analyses (Table S1 and S2). The range of interatomic distances is comparable to those found in other bismuth selenides and tin bismuth selenides (Table S3, visualized as a function of *t* in Figure S9). Crystallographic data[33] are shown in Table S4, structure parameters including modulation parame-

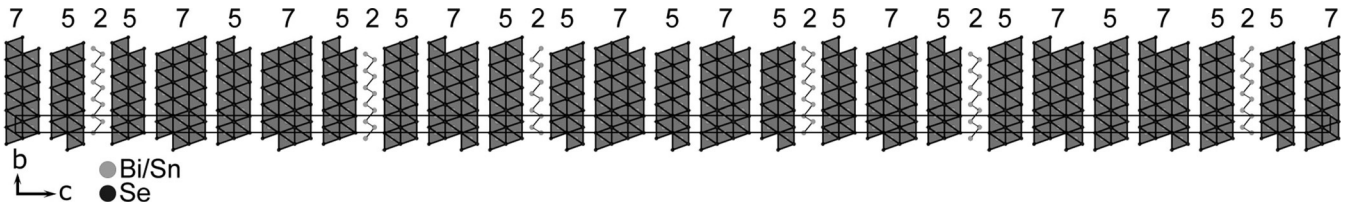

Figure 1. Crystal structure of $Sn_{2.8(4)}Bi_{20.2(4)}Se_{27}$ viewed along [100]: 150*R* stacking sequence of 7525757525|7525757525|7525757525 (cf. text); Se atoms are displayed in black, Bi/Sn atoms in gray; $(Bi,Sn)Se_6$ octahedra are highlighted in order illustrate the different thicknesses of the rock-salt-like slabs; the zigzag lines correspond to $(Bi,Sn)_2$ layers; the unit cell is indicated.

ters are given in Tables S5 and S6 (note that R values for some "satellite orders" are affected by adjacent very strong reflections of other orders and that the intensity does not decrease with increasing "satellite order" as there is no wave-like modulation).

The long-periodic trigonal structure of $Sn_{2.8(4)}Bi_{20.2(4)}Se_{27}$ with a 150*R* stacking sequence is built up from three different kinds of slabs: double and quintuple layers known from the system Bi/Te, an additional septuple layers obtained by the introduction of Sn. The 7525757525|7525757525|7525757525 sequence corresponds to an extremely large lattice parameter of the 3D-periodic structure, which amounts to 282.6 Å. This is the first layered chalcogenide with three different building blocks, and it features by far the longest translation period found in the system Sn/Bi/Se. Taking into account the slabs, the formula can be written as $(Sn_{0.1}Bi_{1.9})_2(Sn_{0.3}Bi_{1.7}Se_3)_5(Sn_{0.4}Bi_{2.6}Se_4)_3$. Assuming Bi^0 and Sn^0 in the double layers and Sn^{2+}, Bi^{3+} and Se^{2-} in the quintuple and septuple slabs, the overall charge of the compound is neutral within standard deviations. Sn/Bi cation disorder in septuple slabs has also nicely been confirmed by X-ray diffraction and Mössbauer spectroscopy of $SnBi_4Se_7$.[34]

A structure model in 3D derived from the description in superspace (Figure 1) can be only be refined tentatively (Table S7) using a 3D dataset. Since such a 3D dataset corresponds to a (3+1)D one with satellite reflections up to the 30th order, the model has too many parameters without a reasonable amount of observed data. Thus, the commensurately modulated description is inevitable although there is no wave-like modulation as known from typical modulated structures. However, the refined atom positions of such a 3D model do not deviate much from those directly derived from the (3+1)D superspace model (Table S8). Referring to the superspace description of bismuth selenides by Lidin et al.,[28] the *q*-vector of 87/50=1.74 can be correlated to the stacking sequence and the resulting number of atom layers in the unit cell (Table S9). STEM-HAADF images (Figure 2) confirm the long-periodic stacking sequence of $Sn_{2.8(4)}Bi_{20.2(4)}Se_{27}$ as derived from the single crystal data. The presence of Sn on all metal atom sites as indicated by the X-ray data corresponds well with aberration-corrected STEM-HAADF and chemical mapping by atomic-resolution EDX. Figure 3 shows a 525 stacking sequence with a double layer in the center (a–d) and a 57 stacking sequence with a van der Waals gap between the two blocks (e–h). Intensities in STEM images and their projection perpendicular [001] further confirm the atom distribution along the sequence (Figure S10). Selected-area electron diffraction (SAED) patterns and Fourier transforms of STEM images along [210] match the diffraction pattern calculated from the 3D model derived from the (3+1)D structure refinement (Figure 4) and thus additionally confirm the lattice parameter of 286.6(6) Å. A further SAED pattern along [100] with the corresponding simulation is shown in Figure S11.

Occasionally, stacking faults and different stacking sequences have locally been observed during extensive electron microscopy studies (Figure S12). Yet, the presented structure is by far the predominant stacking sequence.

In conclusion, repeated annealing afforded $Sn_{2.8(4)}Bi_{20.2(4)}Se_{27}$, a new compound in the system Sn/Bi/Se with an extraordinarily long-periodic 150*R* stacking sequence 7525757525|7525757525|7525757525, resulting in a lattice parameter of $c=282.6(6)$ Å. The structure is built up from three different types of slabs, which significantly expands the plethora of known structure models for layered chalcogenides. In $Sn_{2.8(4)}Bi_{20.2(4)}Se_{27}$, the structural features of binary pnictogen-rich chalcogenides, that is, double and quintuple layers and those of ternary tetradymite-like chalcogenides, that is, quintuple and septuple layers, are combined and lead to the unusual long-range ordering. It remains, however, an open and very intriguing question, why such structures form and why they are seemingly thermodynamically stable. The large unit cell and the mixed occupancies impede theoretical calculations as alternative models with different arrangements of the same building blocks will show only tiny differences in the strength of van der Waals interactions between the slabs. For example, in the related compound $Ge_2Sb_2Te_5$, which features much smaller translation periods, activation energies for transitions between ordered and disordered models, which differ by ca. 1 eV in energy, have been calculated to be as low as 0.005 eV.[35] The structure model was obtained by means of X-ray diffraction using a microfocused synchrotron beam and confirmed by

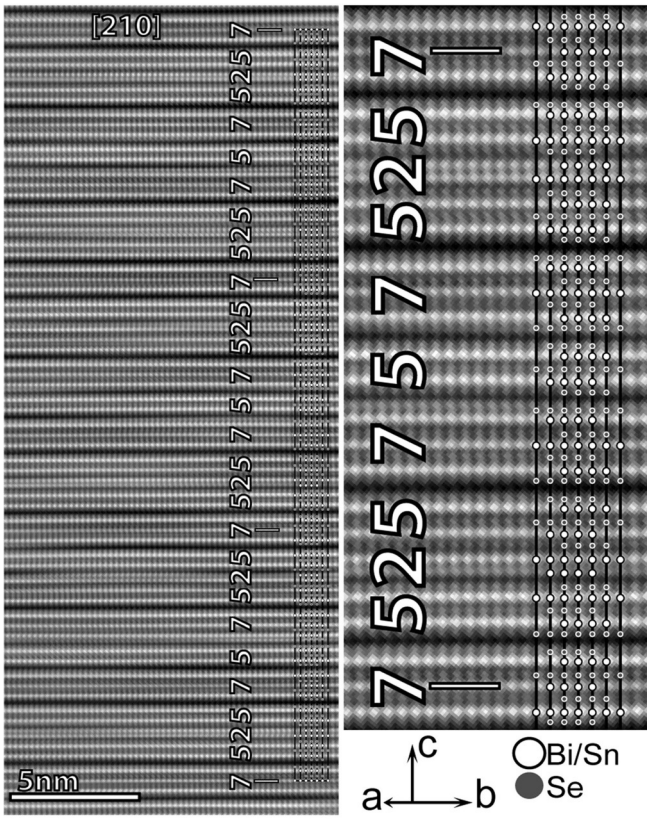

Figure 2. Fourier-filtered STEM-HAADF image (300 kV) along [210] with an image of the crystal structure of $Sn_{2.8(4)}Bi_{20.2(4)}Se_{27}$ in the corresponding projection as an overlay; the asymmetric unit (7525757525 sequence, cf. text) is shown on the right in an enlarged image. In the HAADF images, brighter contrast corresponds to Bi/Sn atom columns and darker contrast to Se atom columns. Se atoms are displayed as gray circles and Bi/Sn as white circles.

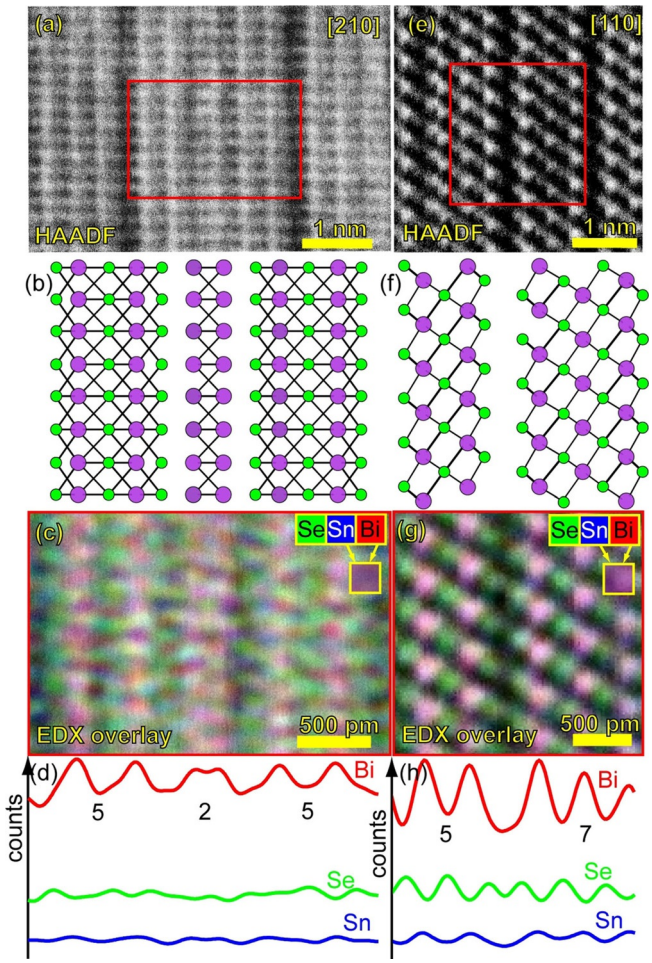

Figure 3. STEM-HAADF images along zone axes [210] (a) and [110] (e), brighter contrast corresponds to Bi/Sn atom columns and darker contrast to Se atom columns; (c, g) EDX maps of the indicated (red box) section of the STEM-HAADF images with (b, f) corresponding structure projections and (d, h) integrated EDX signal projected perpendicular to the layers (projection along [210] or [110], that is, parallel to the layers, Se signals and atoms are highlighted in green and Bi/Sn signals and atoms in red and blue, showing mixed occupancy on all cation positions as indicated by the violet color. (b), (c) and (d) show a 525 stacking sequence with a double layer in the center; (f), (g) and (h) depict a 57 stacking sequence with a van der Waals gap between the two blocks. (a, c) were recorded using 200 kV, (e, g) using 300 kV accelerating voltage.

STEM-HAADF measurements with atomic resolution and EDX mappings. The synergism of these methods enables unprecedented accuracy of structure determinations of microcrystalline compounds and promotes the discovery of numerous new related layered compounds with mixed site occupancies. These may exhibit intriguing physical properties such as thermoelectricity or non-trivial topological behavior.

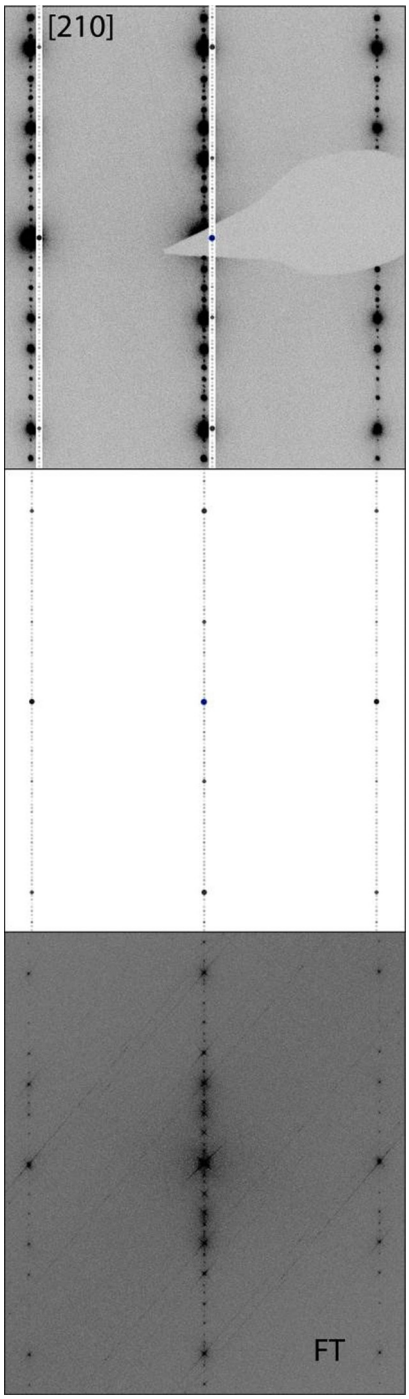

Figure 4. Comparison of an experimental SAED pattern (top, zone axis [210]), a Fourier transform of the STEM-HAADF image displayed in Figure 2 (bottom) with a simulated SAED pattern (middle, based on the structure model from single crystal data); for better comparability, cutouts of the simulation are repeated as insets in the experimental pattern.

Experimental Section

$Sn_{2.8(4)}Bi_{20.2(4)}Se_{27}$ was formed during the decomposition of a quenched sample of $SnBi_4Te_7$[29] upon repeated heating. For TEM measurements, the powdered sample was drop-cast on a copper grid coated with a holey carbon film. This grid was fixed on a glass capillary for single crystal data collection at the European Synchrotron Radiation Facility (ESRF). For STEM measurements, polycrystalline pieces were embedded in epoxy resin and mechanically cut and thinned to a thickness of ≈20 µm in the center using a dimple grinder. Electron transparency was achieved by polishing a hole in the center of the disc by Ar-ion milling (Figure S13). Further details are given in the Supporting Information.

Acknowledgements

We gratefully acknowledge beamtime at the ESRF (project CH-4612) and support by V. Dyadkin (ESRF), P. Schultz and S. Schwarzmüller (both Leipzig University) during data collection. We further thank Prof. Dr. Wolfgang Schnick (LMU Munich) for generous support and valuable comments and Dr. Markus Döblinger for taking care of the TEM and helpful discussions. The Deutsche Forschungsgemeinschaft is acknowledged for financial support (project OE530/3-2). Open access funding enabled and organized by Projekt DEAL.

Conflict of interest

The authors declare no conflict of interest.

Keywords: bismuth · layered compounds · long-periodic crystal structure · selenium · tin

[1] M. G. Kanatzidis, *Inorg. Chem.* **2017**, *56*, 3158 – 3173.
[2] a) T. Zhang, Y. Jiang, Z. Song, H. Huang, Y. He, Z. Fang, H. Weng, C. Fang, *Nature* **2019**, *566*, 475 – 479; b) D. Kong, Y. Cui, *Nat. Chem.* **2011**, *3*, 845 – 849.
[3] Y. L. Chen, J. G. Analytis, J.-H. Chu, Z. K. Liu, S.-K. Mo, X. L. Qi, H. J. Zhang, D. H. Lu, X. Dai, Z. Fang, S. C. Zhang, R. Z. Fisher, Z. Hussain, Z.-X. Shen, *Science* **2009**, *325*, 178 – 181.
[4] a) A. Zeugner, F. Nietschke, A. U. B. Wolter, S. Gaß, R. C. Vidal, T. R. F. Peixoto, D. Pohl, C. Damm, A. Lubk, R. Hentrich, S. K. Moser, C. Fornari, C. H. Min, S. Schatz, K. Kißner, M. Ünzelmann, M. Kaiser, F. Scaravaggi, B. Rellinghaus, K. Nielsch, C. Heß, B. Büchner, F. Reinert, H. Bentmann, O. Oeckler, T. Doert, M. Ruck, A. Isaeva, *Chem. Mater.* **2019**, *31*, 2795 – 2806; b) M. M. Otrokov, I. I. Klimovskikh, H. Bentmann, A. Zeugner, Z. S. Aliev, S. Gaß, A. U. B. Wolter, A. V. Koroleva, D. Estyunin, A. M. Shikin, M. BlancoRey, M. Hoffmann, A. Y. Vyazovskaya, S. V. Eremeev, Y. M. Koroteev, I. R. Amiraslanov, M. B. Babanly, N. T. Mamedov, N. A. Abdullayev, V. N. Zverev, B. Büchner, E. F. Schwier, S. Kumar, A. Kimura, L. Petaccia, G. Di Santo, R. C. Vidal, S. Schatz, K. Kiner, C.-H. Min, S. K. Moser, T. R. F. Peixoto, F. Reinert, A. Ernst, P. M. Echenique, A. Isaeva, E. V. Chulkov, **2018**, arxiv.org/abs/1809.07389.
[5] R. Vilaplana, J. A. Sans, F. J. Manjón, A. Andrada-Chacón, J. Sánchez-Benítez, C. Popescu, O. Gomis, A. L. J. Pereira, B. García-Domene, P. Rodríguez-Hernández, A. Muñoz, D. Daisenberger, O. Oeckler, *J. Alloys Compd.* **2016**, *685*, 962 – 970.
[6] M. Samanta, K. Pal, P. Pal, U. V. Waghmare, K. Biswas, *J. Am. Chem. Soc.* **2018**, *140*, 5866 – 5872.
[7] L.-D. Zhao, S.-H. Lo, Y. Zhang, H. Sun, G. Tan, C. Uher, C. Wolverton, V. P. Dravid, M. G. Kanatzidis, *Nature* **2014**, *508*, 373 – 377.
[8] A. T. Duong, V. Q. Nguyen, G. Duvjir, V. T. Duong, S. Kwon, J. Y. Song, J. K. Lee, J. E. Lee, S. D. Park, T. Min, J. Lee, J. Kim, S. Cho, *Nat. Commun.* **2016**, *7*, 13713.
[9] M. Küpers, P. M. Konze, S. Maintz, S. Steinberg, A. M. Mio, O. Cojocaru-Mirédin, M. Zhu, M. Müller, M. Luysberg, J. Mayer, M. Wuttig, R. Dronskowski, *Angew. Chem. Int. Ed.* **2017**, *56*, 10204 – 10208; *Angew. Chem.* **2017**, *129*, 10338 – 10342.
[10] W.-W. Xiong, J. Miao, K. Ye, Y. Wang, B. Liu, Q. Zhang, *Angew. Chem. Int. Ed.* **2015**, *54*, 546 – 550; *Angew. Chem.* **2015**, *127*, 556 – 560.
[11] M. G. Kanatzidis, *Acc. Chem. Res.* **2005**, *38*, 359 – 368.
[12] J. R. Sootsman, D. Y. Chung, M. G. Kanatzidis, *Angew. Chem. Int. Ed.* **2009**, *48*, 8616 – 8639; *Angew. Chem.* **2009**, *121*, 8768 – 8792.
[13] Y. Feutelais, B. Legendre, N. Rodier, V. Agafonov, *Mater. Res. Bull.* **1993**, *28*, 591 – 596.
[14] N. Frangis, S. Kuypers, C. Manolikas, G. Van Tendeloo, J. Van Landuyt, S. Amelinckx, *J. Solid State Chem.* **1990**, *84*, 314 – 334; note that Amelinckx et al. do not differentiate between possible Te-Bi-Te-Bi-Te-Bi-Bi and a Te-Bi-Te-Bi-Te-Bi-Te sequences and denote both as septuple (7) layers, whereas the nomenclature in this article would call Te-Bi-Te-Bi-Te-Bi-Bi a 52 sequence.
[15] a) L. E. Shelimova, O. G. Karpinskii, V. S. Zemskov, P. P. Konstantinov, *Inorg. Mater.* **2000**, *36*, 235 – 242; b) O. G. Karpinskii, L. E. Shelimova, M. A. Kretova, E. S. Avilov, V. S. Zemskov, *Inorg. Mater.* **2003**, *39*, 240 – 246; c) O. G. Karpinskii, L. E. Shelimova, E. S. Avilov, M. A. Kretova, V. S. Zemskov, *Inorg. Mater.* **2002**, *38*, 17 – 24; d) L. E. Shelimova, O. G. Karpinskii, P. P. Konstantinov, E. S. Avilov, M. A. Kretova, V. S. Zemskov, *Inorg. Mater.* **2004**, *40*, 451 – 460.
[16] N. Frangis, S. Kuypers, C. Manolikas, J. Van Landuyt, S. Amelinckx, *Solid State Commun.* **1989**, *69*, 817 – 819.
[17] R. S. Rai, P. Korgul, G. Singh, *Acta Crystallogr. Sect. B* **1984**, *40*, 132 – 138.
[18] a) I. Kiflawi, S. Mardix, *Acta Crystallogr. Sect. B* **1969**, *25*, 2415 – 2417; b) V. Medizadeh, S. Mardix, *Acta Crystallogr. Sect. C* **1986**, *42*, 518 – 519.
[19] a) B. Pałosz, S. Gierlotka, *Acta Crystallogr. Sect. C* **1983**, *39*, 521 – 528; b) B. Pałosz, S. Gierlotka, *Acta Crystallogr. Sect. C* **1984**, *40*, 1117 – 1119.
[20] B. Pałosz, S. Gierlotka, B. Wiktorowska, D. Dziag, *Acta Crystallogr. Sect. C* **1985**, *41*, 1407 – 1409.
[21] A. F. Wells, *Structural Inorganic Chemistry*, Oxford University Press, New York, **1984**.
[22] R. Terry, D. Vinton, C. D. McMillen, J. W. Kolis, *Angew. Chem. Int. Ed.* **2018**, *57*, 2077 – 2080; *Angew. Chem.* **2018**, *130*, 2099 – 2102.
[23] J. Brugger, T. Armbruster, N. Meisser, C. Hejny, B. Grobety, *Am. Mineral.* **2001**, *86*, 1494 – 1505.
[24] a) J. A. Kohn, D. W. Eckart, C. F. Cook, Jr., *Science* **1971**, *172*, 519 – 525; b) L. A. Kohn, D. W. Eckart, *J. Appl. Phys.* **1965**, *36*, 1171 – 1172.
[25] C. Delacotte, G. F. S. Whitehead, M. J. Pitcher, C. M. Robertson, P. M. Sharp, M. S. Dyer, J. Alaria, J. B. Claridge, G. R. Darling, D. R. Allan, G. Winter, M. J. Rosseinsky, *IUCrJ* **2018**, *5*, 681 – 698.
[26] I. Orlov, L. Palatinus, A. Arakcheeva, G. Chapuis, *Acta Crystallogr. Sect. B* **2007**, *63*, 703 – 712.
[27] L. Elcoro, J. M. Perez-Mato, R. L. Withers, *Acta Crystallogr. Sect. B* **2001**, *57*, 471 – 484.
[28] H. Lind, S. Lidin, *Solid State Sci.* **2003**, *5*, 47 – 57.
[29] F. Heinke, P. Urban, A. Werwein, C. Fraunhofer, T. Rosenthal, S. Schwarzmüller, D. Souchay, F. Fahrnbauer, V. Dyadkin, G. Wagner, O. Oeckler, *Inorg. Chem.* **2018**, *57*, 4427 – 4440.
[30] J. Takagi, Y. Takéuchi, *Acta Crystallogr. Sect. B* **1972**, *28*, 649 – 651.
[31] a) G. B. M. Vaughan, J. P. Wright, A. Bytchkov, C. Curfs, C. Gundlach, M. Orlova, L. Erra, H. Gleyzolle, T. Buslaps, A. Götz, G. Suchet, S. Petitdemange, M. Rossat, L. Margulies, W. Ludwig, A. Snigirev, I. Snigireva, S. Schmidt, H. O. Sørensen, E. M. Lauridsen, U. L. Olsen, J. Oddershede, H. F. Poulsen, *Proc. 31st Risø Int. Symp. Mater. Sci.* **2010**, *521*, 457 – 476; b) F. Fahrnbauer, T. Rosenthal, T. Schmutzler, G. Wagner, G. B. M. Vaughan, J. P. Wright, O. Oeckler, *Angew. Chem. Int. Ed.* **2015**, *54*, 10020 – 10023; *Angew. Chem.* **2015**, *127*, 10158 – 10161; c) P. Bielec, R. Nelson, R. P. Stoffel, L. Eisenburger, D. Günther, A.-K. Henß, J. P. Wright, O. Oeckler, R. Dronskowski, W. Schnick, *Angew. Chem. Int. Ed.* **2019**, *58*, 1432 – 1436; *Angew. Chem.* **2019**, *131*, 1446 – 1450.
[32] M. M. Stasova, *J. Struct. Chem.* **1967**, *8*, 584 – 589.
[33] Superspace group $R\bar{3}m(00\gamma)00$, $a = 4.1819(4)$, $c = 5.6528(5)$ Å, $V = 85.61(1)$ Å^3, $Z = 3$, $\rho_{diff} = 7.7857$ g cm^{-3}, $R1$ (all data) $= 0.0451$, $R1$ [$I > 2\sigma(I)$] $= 0.0446$, wR (all) $= 0.0699$, wR [$I > 2\sigma(I)$] $= 0.0678$, $R_{int} = 0.0310$, $R_\sigma = 0.054$, 12 parameters for 6375 reflections (411 independent). 3D model: space group $R\bar{3}m$, $a = 4.1819(4)$, $c = 282.64(6)$ Å. Further details of the crystal structure investigations are given in the Supporting Information. Deposition number 1949450 contains the supplementary crystallographic data for this paper. These data are provided free of charge by the joint Cambridge Crystallographic Data Centre and Fachinformationszentrum Karlsruhe Access Structures service.
[34] C. Pérez Vicente, J. L. Tirado, K. Adouby, J. C. Jumas, A. Abba Touré, G. Kra, *Inorg. Chem.* **1999**, *38*, 2131 – 2135.
[35] S. He, L. Zhu, J. Zhou, Z. Sun, *Inorg. Chem.* **2017**, *56*, 11990 – 11997.

Manuscript received: February 6, 2020
Accepted manuscript online: March 27, 2020
Version of record online: July 27, 2020

